NET CAPTURING OF TUMBLING SPACE DEBRIS: CONTACT MODELLING EFFECTS ON THE EVOLUTION OF THE DISPOSAL DYNAMICS

R. Benvenuto [(1)], S.Salvi [(2)], M. Lavagna[(3)]

[(1)]Politecnico di Milano, Dept. Of Aerospace Science and Technologies, Via La Masa 34, 20156, Milano, Italy, Email: riccardo.benvenuto@polimi.it
[(2)]Politecnico di Milano, Dept. Of Aerospace Science and Technologies, Via La Masa 34, 20156, Milano, Italy, Email: samuele.salvi@mail.polimi.it
[(3)]Politecnico di Milano, Dept. Of Aerospace Science and Technologies, Via La Masa 34, 20156, Milano, Italy, Email: michelle.lavagna@polimi.it

ABSTRACT

Debris removal in Earth orbits is an urgent issue to be faced for space exploitation durability. A general-purpose removal system design should effectively intervene on objects different in configuration, materials and possibly in dimensions. Moreover, targets to be captured do not cooperate and have a complex, free, not completely known dynamics. For these reasons, among different proposed techniques to actively remove debris from orbit, tethered-nets present appealing benefits by capturing debris from a safety distance and by establishing a flexible tethered connection between the chaser and the target.
In the paper, through the exploitation of a multibody dynamics simulation tool, critical phases as wrapping and towing are analysed to address the tethered-stack controllability. It is shown how the role of contact modelling is fundamental to describe the coupled dynamics: it is demonstrated how friction between the net and a tumbling target allows reducing its angular motion, stabilizing the system and allowing safer towing operations.

1. INTRODUCTION

Space debris mitigation and remediation are urgent and growing issues to be faced for the future of space operations and exploitation durability [1], [2]. In past decades, several launches have placed more than 6000 satellites into orbit, of which less than a thousand are still operational today. The Active Debris Removal (ADR) topic focuses on trading-off, designing and building up mechanisms to be mounted on-board an active chaser satellite that can rendezvous, capture and dispose of uncooperative tumbling target spacecraft.
Nowadays the European community, working on large space debris active removal methodologies, accomplished feasibility and phase A studies focused on setting the system requirements and addressing the most promising techniques to be further investigated up to the final implementation [3]. Among them, the use of throw-nets and tow-tethers has been advocated as one of the preferred solutions [4]: a flexible capture net is cast from an active satellite by impulsively accelerating a number of flying weights, hereinafter named bullets, attached to the net mouth; then the relative trajectory of the bullets deploys the capture net gradually during the flying process; finally the net wraps the debris element, closes around it and thanks to the active chaser, tethered connected with the net, drag it to the disposal location in space. The concept of tethered-net satellite capture is represented in Fig. 1.

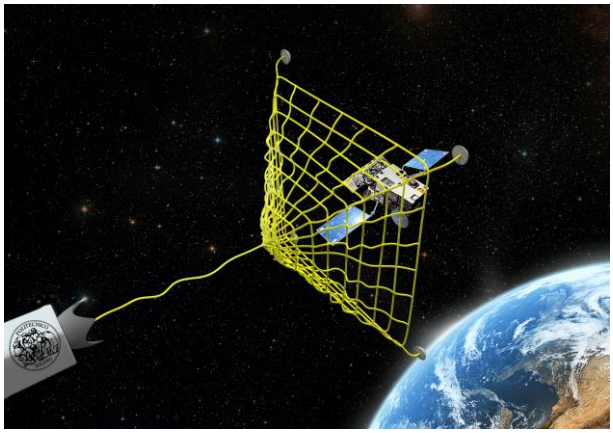

Figure 1. Tethered-net capture concept

The greatest advantages of tethered-net solutions with respect to rigid capture mechanisms are traceable in the higher interfaceability towards unknown targets' physical and dynamics characteristics, isotropic loads and safer capturing distances. They also allows not considering the centre of gravity alignment with thrust axis as a constraint, as it is for any rigid link solution. On the other hand, these techniques are characterized by the difficulty in robustly detect the capture and closure occurrence after the impact and by settling a flexible tethered connection between the chaser and the target. The latter opens new challenges for guidance navigation and control (GNC) design: the chaser GNC system is required to be precise enough to gain stabilized specific relative orbits and to robustly perform de/re-orbiting operations, while controlling a complex system and damping vibrations of flexible elements and connections.
This paper aims at characterizing the dynamics of such

a complex multibody system during capture and disposal phases, by focusing in particular on the fallouts of different contact models on the stack behaviour and controllability. A dedicated numerical tool has been developed at Politecnico di Milano, Department of Aerospace Science and Technologies (PoliMi-DAER), to simulate the entire composite dynamics, in order to support the overall system design and to synthetize more reliable and adapted GNC laws. The software has been verified and validated through benchmarking with analytical and experimental results. The analysis results, presented in this paper, show the great role played by the contact modelling in the dynamics evolution: a simplified model where no slippage or friction is present is compared to a refined model where fine collision detection and contact laws are implemented. Both models exploit the same discretized viscoelastic laws to describe the tethered-net flexible dynamics, however the simplified model reduces the net to some tethers firmly attached to the target body. A tumbling target capture and towing is simulated using both models: in the first case, the evolution of target angular velocity shows the so-called tail wagging effect, i.e. the periodic oscillation of the debris which appears as a stable limit cycle obtained after a short transient during towing. On the other hand, the complete refined net model allows appreciating the higher fidelity to the physics of the phenomenon: a modified Coulomb friction law is also introduced and discussed. The introduction of friction, causing energy dissipation thanks to the relative motion of the target debris inside the net, allows demonstrating how the energy dissipated through contact and slippage is able to reduce the angular momentum of the tumbling target, passively damping its angular motion.

In section 2, the multibody dynamics simulation environment is presented, detailing the mathematical models of both viscoelastic flexible dynamics and contact dynamics. In section 3 simulations results are shown and the comparison with the simplified model is presented. Finally, in section 4 conclusions are drawn.

2. MULTIBODY DYNAMICS SIMULATION ENVIRONMENT

In this section, the multibody dynamics simulation environment is presented. The tool has been developed in house at PoliMi-DAER, to reliably model the dynamics of tethered-net ADR systems and effectively serve as a tool to support system design and to allow control laws implementation, testing and validation.

To guarantee good performances in terms of computational time, lumped parameters methods have been chosen. These models also allow:

- to describe net large deformations and to only include positive tension on the tethers, due to the inability of net's material to withstand compression;
- to tune the accuracy by modifying the number of discretizing elements;
- to parametrically treat different materials and exploit ad-hoc viscoelastic laws;
- to treat general net topologies and configurations, both folded and deployed;
- to obtain a system of explicit ordinary differential equations (ODE).

The chaser and the target are modelled as six degrees of freedom bodies, as well as the bullets, through Newton's and Euler's laws for translational and rotational dynamics. All reactions on bodies due to tethered-net system are taken into account.

The system dynamics are subject to the full range of forces and torques expected in Earth orbit. Dealing with these systems, it is important to precisely model the environmental effects: in particular the gravity and its gradient are important when dealing with long tethers. The atmospheric density also plays an important role both for its increasing magnitude during de-orbit and for its gradient along long tethers or large nets.

The spatial motion of the system is studied in non-uniform Earth gravity field, under the action of chaser de-orbiting thrusters (when applicable), aerodynamic drag and solar pressure, which are taken into account as external perturbations on all the elements composing the system, both flexible and rigid. In [5], a description of the environmental model and the drag modelling on flexible elements is reported.

The simulator has been implemented in Matlab/Simulink, and the obtained large system of ODE is solved by exploiting the software's built-in integration capabilities, with Runge-Kutta methods, after auto-coding it in C++ to improve time performances.

2.1 Viscoelastic model

The simplest and yet most efficient way to describe a flexible body, that does not withstand compression, is to model it as series of point masses connected by springs-dashpots: the constitutive law of the material can be modelled through the combination of spring-dampers resulting in different tension laws. In Fig. 2 the discretization of a planar net is depicted along with a representation of the tether physical model, each net's thread being modelled as a tether.

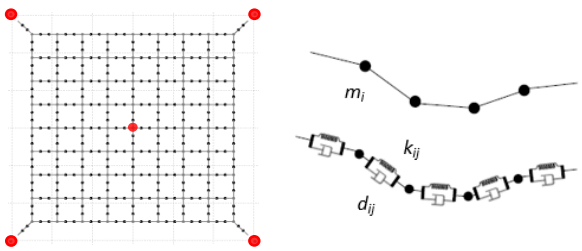

Figure 2. Tethered-net model and discretization

The linear Kelvin-Voigt model has been chosen here

because of the direct relationship of its coefficient with material mechanical properties. Tension on rope elements can be expressed as in (1):

$$T_{i,j} = \begin{cases} \left[-k_{ij}\left(|R_{ij}| - l_{nom}\right) - d_{ij}\left(V_{ij} \bullet \hat{R}_{ij}\right)\right]\hat{R}_{ij} & if\,|R_{ij}| > l_{nom} \\ 0 & if\,|R_{ij}| \le l_{nom} \end{cases} \quad (1)$$

where k_{ij} and d_{ij} are the elastic and viscous parameters of element ij (i.e. between node i and j), l_{nom} is the nominal un-stretched length of the tether element, R_{ij} and V_{ij} are, respectively, the relative position and velocity between two consecutive masses (the hat indicating the normalized vector). The stiffness is directly related to material and rope properties, being the axial stiffness defined as in (2):

$$k_{ij} = \frac{EA}{l_{nom}} \quad (2)$$

where E is the Young's modulus and A the tether cross section. The damping is directly related to the tether mass and natural frequency through its damping ratio ξ as in (3):

$$d_{ij} = 2\xi\sqrt{m_{ij}k_{ij}} \quad (3)$$

Damping ratio and Young's Modulus have been determined experimentally at PoliMi-DAER premises for different synthetic fibre ropes that are suitable candidate for these particular ADR systems and meet the requirements on strength and stiffness.

2.2 Contact dynamics model

Multiple contact events are expected to occur during capture and wrapping phases, both among different parts of the net and between the net and the target. As a result, the representation of the effect of contacts between the bodies is a key to the fidelity of the simulation to reality.

A hierarchical bounding-boxes collision detection algorithm, as developed in [6], has been set-up. It consists of an n-phases algorithm refining the zone of contact, in order to select the specific subsystems of discretization nodes to be cross-checked for collision. The control boxes considered are minimum spherical bounding boxes (MSBB), as detailed in [7]. The selected MSBB method allows a fast and precise treatment of the impact of the net with borders and edges; Furthermore, it well adapts to the discretization of the net/threads in point masses, allowing a simple management of collision detection and contact algorithms.

Many approaches are available to model contact dynamics [8]. Here a regularized contact models has been adopted: the regularization consists in the reformulation of the problem, changing the nature of the impact from a discontinuous process into a continuous one. The contact forces are described as a function of the contact deformation by smothering the discontinuity of the impact and friction forces in the constraints. This approach is also referred as "penalty method", since the model returns a measure of the constraint violation, the larger the violation, the higher the penalty. In contrast to the contact models based on the rigid body assumption, compliant models describe the rate-dependent normal and tangential compliance relations over time. These models can be easily integrated within the simulation environment based on ODE solvers and the formulation provides the required degree of freedom necessary to regulate and adjust the contact parameters according to the experimental results.

Furthermore, a point contact model theory is valid as long as the contact region is small, compared to the dimensions of the colliding bodies, and this holds for the aforementioned net modelling. The contact model takes the form of a lumped-parameter spring, as represented in Fig. 3.

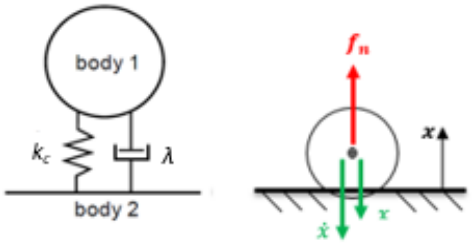

Figure 3. Model representation scheme for normal contact force

Therefore, the local deformation can be parameterized as a function of the penetration depth between the non-deformed bodies. This produces a single algebraic expression relating the inter-penetration to the normal contact force. For direct central frictionless impacts**,** Hunt and Crossley has proven to be a valid contact model [9], which integrate the Hertz theory (spring model) with a damper in order to take into account the energy dissipation in the impact normal direction. The compliant normal-force expression, proposed by Hunt and Crossley for direct central and frictionless impact, is a non-linear spring-damper model, as in (4):

$$F_n = -k_c x^n - \lambda x^n \dot{x} \quad (4)$$

where:

- k_c is the equivalent stiffness (Eq. 5).
- n is an empirically coefficient related to the impacting geometries [10];
- x and $\dot{x}$ are respectively the penetration depth and velocity;
- λ is the hysteresis damping factor.

This damped model is consistent with the expectation that the total contact force should vanish whenever the penetration depth goes to zero. This means that no impulsive behaviour of the contact force dynamics appears at impact. As visible in Fig. 4 on the left, in the case of a linear spring-damper model (such as Kelvin-Voigt, as in (1)), the contact force is non-null at contact occurrence even with null penetration, negative at the end of the impact phase. This behavior contradicts two characteristics that are expected from a consistent model:

- contact force equal to zero at zero-penetration;
- contact force always positive, to avoid *sticking* effect.

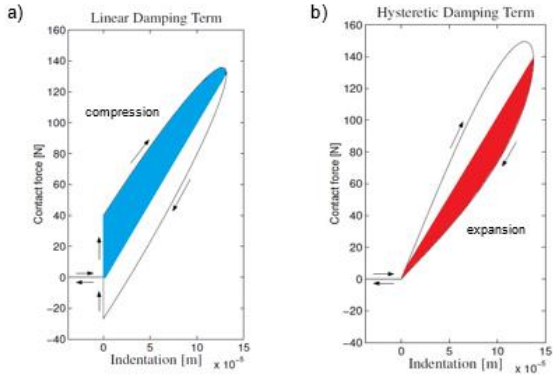

Figure 4: Linear vs. hysteretic damping in normal contact force model

Assuming that the energy dissipated (area inside the loop) during the compressive phase (blue) and the one dissipated during the expansion phase (red) are equal, Hunt and Crossley approximate the hysteresis damping factor as in (5):

$$\lambda = \frac{3}{2}\alpha \; k_c \tag{5}$$

where α is an experimental parameter that usually varies in the range [0.08-0.32] s/m and relates the coefficient of restitution e to the impact initial normal velocity as in (6):

$$e = 1 - \alpha \; v_n^{\,i} \tag{6}$$

Finally, in order to define the contact stiffness coefficients, a few reasonable assumptions were made: first, all contacts are supposed to be elastic; second, the nodes of the net are approximated to spheres consistently with the collision detection algorithm discretization; finally, the debris is expected to be much bigger than each node of the net, therefore the contact between net and debris can be thought as the result of multiple contacts among a sphere and a plane. As a consequence, apart from some special cases (e.g. a node impacting a corner of the debris), impact happens between two continuous and non-conforming surfaces, which make first contact at a point and for which the resulting stresses are highly concentrated. Within these assumptions, Hertzian contact theory is valid and it is possible to use the well-known results [10] summarized below in (7) and (8), where r is the sphere radius.

$$k_c = \frac{4}{3\pi} \frac{\sqrt{r}}{h_1 + h_2} \tag{7}$$

$$h_i = \frac{1 - \nu_i^{\,2}}{\pi \; E_i} \tag{8}$$

According to Hertzian theory, n appearing in (4) is equal to 1.5.
Contact model implementation has been verified by simulating simpler test cases. Results have proven to be coherent with theory and the physics of the phenomenon, i.e. the contact force is always positive and non-impulsive and the total energy (including the dissipated part) is conserved.

2.3 Friction model

A regularized version of the Coulomb's law of dry friction has been adopted: the proposed semi-empirical model is based on the so-called "Dwell Time Dependency" theory of friction, which theorizes a time depending behaviour of stiction forces below a velocity threshold.
It is called static friction or stiction, the one occurring below a force threshold proportional to the acting normal contact force F_n, according to the Coulomb's static friction coefficient μ_s as in (9):

$$F_t \le \mu_s |F_n| \tag{9}$$

Experimental observations [11] have shown that the full magnitude of the stiction force does not come into effect as soon as the relative velocity becomes zero. Instead, the maximum static friction force gradually increases over time and eventually reaches its upper limit.
The important advancement in this theory is the conversion of the force-based transition from static to dynamic, into a velocity threshold definition [12]. Calling v_t the tangential velocity modulus and v_s the velocity threshold, the friction force modulus F_t is defined in (10):

$$F_t = \begin{cases} \mu_d |F_n| & if \;\; v_t \ge v_s \\ \mu_d |F_n| \dfrac{v_t}{v_s}\left(2 - \dfrac{v_t}{v_s}\right) & if \;\; v_t < v_s \end{cases} \tag{10}$$

Here, μ_d is the Coulomb's dynamic friction coefficient. It is a regularized version of the Coulomb's law of dry friction: if the slip velocity falls below the threshold v_s,

the friction force is faded out quadratically, as represented in Fig. 5.
As a first guess, transition velocity v_s (to be correctly tuned by experimental tests) was set equal to the Stribeck velocity that is the velocity at which the stick-slip effect occurs (in the Stribeck curve). It has been proven experimentally [13] that a velocity threshold in the range between 10^{-4} and 10^{-6} m/s is a good compromise between the accuracy and computational effectiveness.

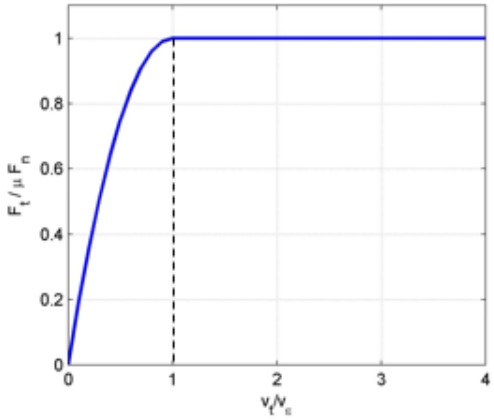

Figure 5. Regularized version of Coulomb's friction law

By definition, the acting direction of the friction force is always tangent to the surface and opposite of the relative velocity between the two sliding bodies.

3 SIMULATION RESULTS

3.1 Reference scenario

In order to analyse the contact model and to clearly identify the fall-outs on system dynamics, the following simulations have run with a simplified cubical target without appendages or antennas.
The following simulations refer to a scenario of an In-Orbit Demonstration (IOD) mission, envisaged to increase the technology readiness level (TRL) of net capturing systems. For this reason the system has been dynamically scaled down with respect to a large satellite capture.
In order to limit system masses and volumes, while meeting the requirements on strength and debris generation containment, nets are designed with reinforced perimeter and some internal threads (medians or diagonals) directly linked to the tether, to withstand pulling loads. The secondary threads have a decreased diameter and have function of both containment and motion damping through friction, as explained in the following paragraphs.
The net is provided with a closing mechanism: an interlaced thread on the net perimeter (e.g. its mouth) is wounded by reels inside the bullets to close the net mouth around the target. The closing mechanism is activated at impact occurrence with a delay depending on the net velocity and target features and it guarantees a safe and firm grasping during towing. More details on the net closing mechanism can also be found in [7]. As an example, a conical net with 8 bullets and a closing mechanism is represented in Fig. 7 with a detail on its closing mechanism.

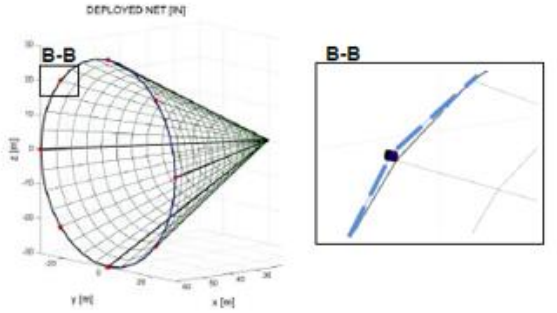

Figure 7. Conical net with 8 bullets and a closing mechanism (zoom on one bullet and closing threads in blue)

3.2 Tumbling target capturing: wrapping and closure phases

In Tab. 1 the simulation parameters are reported.

Table 1: Simulation parameters

	Planar Net	**Conical Net**
Size [m]	2x2	2x2x2
Mesh [m]	0.2	
Bullets # [-]	4	8
Bullet Mass [kg]	0.07	0.02
Bullet ejection velocity [m/s]	2	
Divergence angle [deg]	30	
Net mass [kg]	0.14	0.16
Threads material	Technora	
Threads diameter [mm]	2 / 0.5	
Threads Young's Modulus [GPa]	25	
Threads damping factor [-]	0.3	
Equivalent contact stiffness [N/m]	500	
Hysteresis damping factor [-]	0.5	
Friction factor [-]	0.1	
Target size [m]	0.5x0.5x0.5	0.5x1x0.5
Target angular velocity [deg/s]	[1 -5 1]	
Capture distance [m]	2.5	2.5
Orbit	SS0 500 km	

In Fig. 8 the planar net is represented in both deployed and folded configurations. The conical net is represented in Fig. 7.

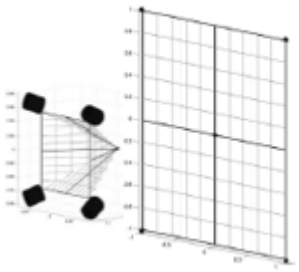

Figure 8. Planar net with 4 bullets and square mesh, folded and deployed configurations

Fig. 9 depicts the capture sequence for the planar net while Fig. 10 shows the capturing simulation output for the conical net case. The reference system is the Local Vertical Local Horizontal (LVLH), centred on the chaser; the capture and pulling is executed along V-bar.
By analysing simulations results, the following considerations are possible:

- conical and planar nets have different capturing behaviours: while the planar net mainly relies on impact and wrapping, three-dimensional nets, such as the conical one, envelope the target not necessarily impacting with it. Therefore it is possible to conclude that the second type of capturing is safer and more reliable but on the other hand it requires much bigger nets (the target needs to be totally enveloped), with obviously an increase in masses and volumes.
- The closing mechanism, as it is simulated, has proven to be effective. However, experimental tests are needed to tune the design, characterize performance and verify functionalities.

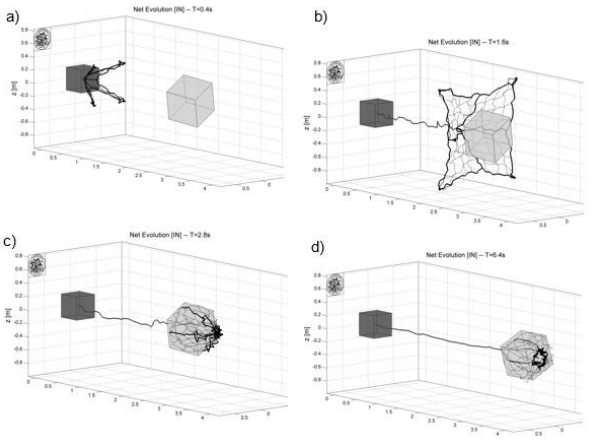

Figure 9. Planar net capture sequence

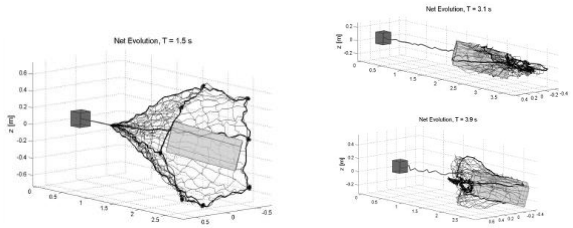

Figure 10. Conical net capture sequence

3.3 Pulling phase: comparison with a non-slipping simplified model

Finally, a comparison with a non-slipping simplified model is presented to better appreciate the effects of contact modelling on the evolution of disposal dynamics.
The simplified model, presented in [14], is a reduced model that avoids the complexity of the contact dynamics, fixing directly a discrete number of contact points on the Target. The net is reduced to a number of tethered-links equal to the number of the connection points and fixed to the target at one end and to the tether at the other. This simplified numerical tool has been built up specifically to design disposal control laws, since running faster than the detailed model including contact. The entire capture dynamics cannot be simulated and the simulation starts with the two objects already connected. The net exploited is the first in Tab. 1. The Target considered is a 0.5 m cube of 83 kg, tumbling at [1 -5 1] deg/s. The thrusting law considered is a single continuous burn of 15 N for a time of 400 seconds.
Fig. 11 reports the simplified model in its initial condition at the beginning of pulling phase.

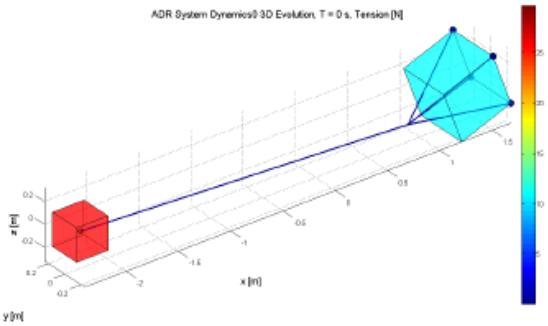

Figure 11. Reduced model initial configuration

Fig. 12, depicts the target-chaser relative distance and the tension on tether and net elements for the simplified model. It is possible to remark a very modest initial bouncing dynamics, due to the simplified initial conditions and missing capture phase.
Fig. 13 shows the target-chaser relative position and velocity in LVLH frame, while Fig. 14 highlights the tensions on tether and net elements; both figures refer to the complete model case . More accurate and reliable

dynamics results are obtained exploiting the complete numerical tool described so far in this work. The thrusting phase is extended to 400s to better appreciate the dynamics evolution. Besides the initial bouncing of the target towards the chaser, involving stresses overshooting and oscillations, the final forces stabilize and the exact thrusting action can be clearly visible in the tether transmitted force. The initial overshoot is due to the tether tensioning after the capture: these dynamics are absent in the simplified model. However, the initial bouncing, due to the initial shock, is then completely damped after 100 seconds, as it is evident from Fig. 13.

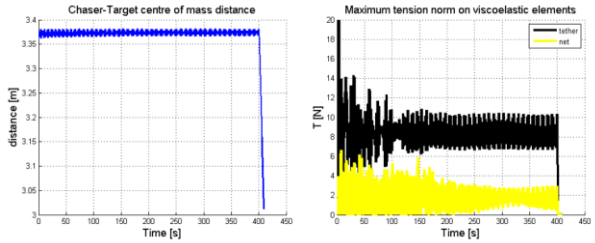

Figure 12. Simplified model simulation results: a) Target-Chaser relative distance, b) maximum net (yellow) and tether (black) tensions

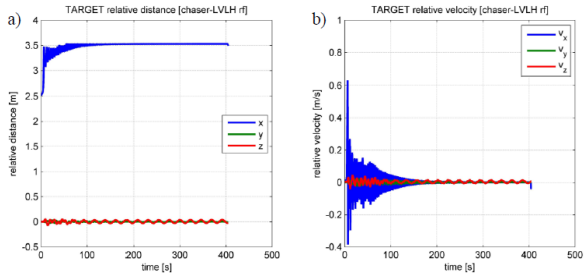

Figure 13. Complete model simulation results: Target-Chaser relative a) position and b) velocity

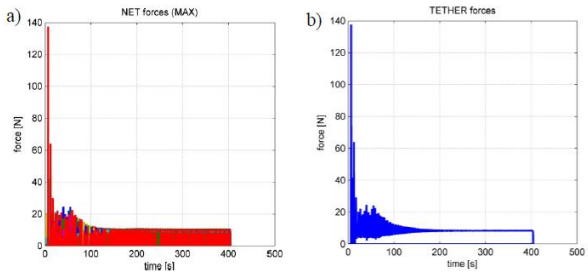

Figure 14. Complete model simulation results: forces acting on a) Net and b) Tether during capture and disposal phases

By analysing contact forces and torques transmitted to the target by the net, represented in Fig. 15, it is possible to note that, coherently with the physics of the pulling, the transmitted action is mainly along V-bar (F_x), while the other components are damped during towing.

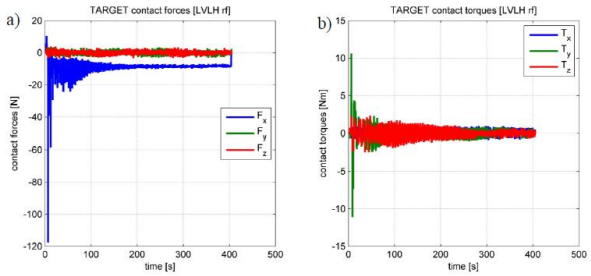

Figure 15. Complete model simulation results: Target acting contact a) forces and b) torques

Finally, it is possible to appreciate the contact model indirect effects, involving energy dissipation through slippage and friction: in Fig. 16 the target body angular velocities are reported for both the simplified and complete model. In the first case, i.e. the simplified model, the evolution of target angular velocity shows the so-called tail wagging effect, i.e. the periodic oscillation of the debris which appears as a stable limit cycle obtained after a short transient during towing, whose values are much bigger than the initial one. After shutting down thrusters the target motion continues freely. This behaviour would be dangerous to carry out the operations both during pulling and during post-burn phases, risking entanglement with the tether, its breakage and possibly leading to chaser control authority loss. On the other hand, in the complete model case, the initial angular velocities and the further speeding-up contribution due to the initial shock torques are clearly dissipated, proving the theorized effectiveness of the passive damping effect of tether-net capturing and demonstrating the importance of contact dynamics laws for the evolution of the overall dynamics.

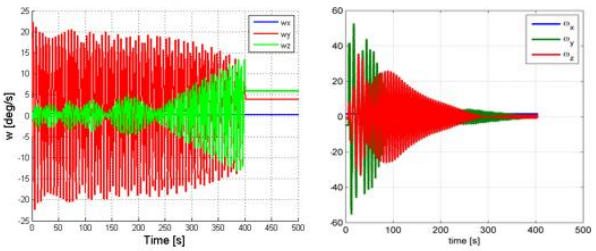

Figure 16. Target angular velocities in body frame: a) simplified model, b) complete model

Finally, in Fig. 17 the final configuration after 400 seconds pulling is showed.

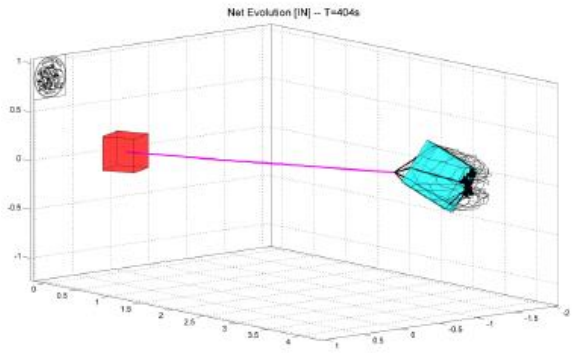

Figure 17. Final time frame of simulated dynamics, after 400s of thrusting.

4 CONCLUSIONS

In this paper, a complete and physically-based mathematical model of a tethered-net device for active space debris removal is presented. The main goal of this simulator is to support the design of such flexible ADR system: it revealed to be a useful tool to describe the overall dynamic behaviour and the unforeseen dynamics arising from the interaction between two isolated bodies, becoming a single multibody system to deorbit. In particular, most of the attention was put on the interface between the net and the free-tumbling object during the disposal pull.

Results have shown the great role played by the contact modelling, proving energy dissipation and therefore reducing both the axial bouncing dynamics of the target during the pull and the target angular momentum content.

These translate into a major benefit for the net-device concept, providing a passive damping aid. This effect is extremely important from a control point of view, helping the stabilization of the stack: it is demonstrated how the passive angular motion damping allows the chaser to keep the control authority during the most delicate phases of the mission.

By providing a passive stabilization of the stack during disposal, reducing the tail-wagging effect and allowing multi-burn disposal strategies, tethered-net devices appear to be promising, presenting the most benefits with respect to other proposed ADR strategies, as demonstrated by an advanced simulation environment.

5 REFERENCES

1. Liou J.C. & Johnson N.L. (2007), *A sensitivity study of the effectiveness of active debris removal in LEO*, in Proc. 58th IAC 'International Astronautical Congress' (IAC-07-A6.3.05), Hyderabad, India.
2. Bastida B. & Krag H. (2011), *Analyzing the criteria for a stable environment*, in Proc. 2011 AAS/AIAA Astrodynamics Specialist Conference, Girdwood, Alaska.
3. Wormnes K., Le Letty R., Summerer L., Schonenborg R., Dubois-Matra O., Luraschi E., Cropp A., Krag H. & Delaval J. (2013), *ESA technologies for space debris remediation* in Proc. 6th European Conference on Space Debris, Darmstadt, Germany.
4. Wormnes K., De Jong J.H., Krag H. & Visentin G. *Throw-nets and tethers for robust space debris capture*, in Proc. 64th IAC 'International Astronautical Congress' (IAC-13-A6.5), Beijing, China.
5. Benvenuto R. & Lavagna M. (2014), *Towing tethers to control debris removal dynamics*, in Proc. 65th IAC 'International Astronautical Congress (IAC-14-C1.6.09), Toronto, Canada.
6. Zachmann G. (2000), *Virtual reality in assembly simulation – Collision detection, simulation algorithms and interaction techniques*, PhD thesis, Department of Computer Science, Darmstadt University of Technology.
7. Benvenuto R., Salvi S. & Lavagna M. (2015), *Dynamics analysis and GNC design of flexible systems for space debris active removal*, Acta Astronautica,http://dx.doi.org/10.1016/j.actaastro.2015.01.014i.
8. Gilardi G. & Sharf I. (2002), *Litterature survey of contact dynamics modelling*, Mechanism and Machine Theory, Vol. 37, No. 10, pp. 1213-1239.
9. Hunt K. & Crossley H. (1975). Coefficient of restitution interpreted as damping in vibroimpact. Transactions of the ASME Journal of Applied Mechanics.
10. Johnson K.L. (1987), *Contact Mechanics* Cambridge University Press, London.
11. Rabinowicz E. (1956), *Stick and slip*, Scientific American.
12. Hippmann G. (2003), *An algorithm for compliant contact between complexly shaped surfaces in multibody dynamics*, Multibody Dynamics, Jorge A.C. Ambrosio (Ed.).
13. Wojewoda J., Stefański A., Wiercigroch M. & Kapitaniak T. (2008), *Hysteretic effects of dry friction: modelling and experimental studies*, Philosophical Transactions of the Royal Society A: Mathematical, Physical and Engineering Sciences.
14. Benvenuto R., Lavagna M., Cingoli A., Yabar C. & Casasco M. (2014), *MUST: multibody dynamics simulation tool to support the GNC design for active debris removal with flexible elements*, In Proc. 9th International ESA Conference on Guidance, Navigation & Control Systems, Porto, Portugal.